FPCM-9 (2008)
The 9th International Conference on Flow Processes in Composite Materials
Montréal (Québec), Canada
8 ~ 10 July 2008

BIO-BASED THERMOSET POLYMER NANOCOMPOSITES

T.-D. Ngo [1], W. Leelapornpisit [2], M.-T. Ton-That [1, 3], K. C. Cole [1], M. Sepehr [1]

[1] *National Research Council Canada, Industrial Materials Institute (IMI), 75 De Mortagne Blvd., Boucherville, Quebec, Canada J4B 6Y4*
[2] *Department of Mechanical & Industrial Engineering, Concordia University, 1455 De Maisonneuve Blvd., Montreal, Quebec, Canada H3G 1M8*
[3] *Corresponding author's Email: Minh-tan.Ton-that@imi.cnrc-nrc.gc.ca*

ABSTRACT: Bio-based thermoset nanocomposites reinforced with nanoclay particles have been studied. Epoxidized soyabean oil (ESO), a bio-based material, was used as a neat epoxy resin for this study. The ESO was cured with two different types of hardener, namely hexahydrophthalic anhydride and boron trifluoride monoethylamine. Montmorillonite clay, Cloisite Na^+, and organoclays treated with different intercalants, including Nanomer I30E (treated with a long-chain primary amine intercalant), Cloisite 20A, and Cloisite C30B (treated with a quaternary ammonium intercalant), were used in this study. The nanocomposites' rheology, curing characteristics, and morphologies were determined by various techniques, including differential scanning calorimetry (DSC), X-ray diffraction (XRD), and scanning electronic microscopy (SEM). The results indicate that the level of intercalation of the nanoclays is quite distinct. The presence of nanoclay results in a significant increase in hardness of the nanocomposites cured with hexahydrophthalic anhydride, but not of those cured with boron trifluoride monoethylamine. Nanoclay also does not have a strong effect on the T_g of ESO.

KEY WORDS: ESO, bio-based thermoset, nanoclay, nanocomposites

INTRODUCTION

Natural oils, which can be derived from both plant and animal sources, are abundantly found in all parts of the world, making them an ideal alternative chemical feedstock. These oils are predominantly made up of triglyceride molecules, which have a 3-armed star structure. Triglycerides are composed of three fatty acids joined at a glycerol juncture. Most common oils contain fatty acids that vary from 14 to 22 carbons in length, with 0 to 3 double bonds per fatty acid. Besides their application in the food industry, triglyceride oils have been used quite extensively to produce coatings, inks, plasticizers, lubricants, and other agrochemicals [1-7].

Within the polymer field, the application of these oils to toughen polymer materials has been investigated. Because of environmental concerns, the commercial utilization of biological polymers has become the subject of active research during recent decades [8, 9]. Bio-based polymeric materials from renewable resources are of significant importance from both industrial and economic viewpoints. Soya bean oil is a renewable raw material for a wide variety of industrial products, including inks, plasticizers, and paints. The range of potential applications can be expanded by genetic improvements that alter the fatty acid composition of soybean oil. In the past, ESO was mainly used as plasticizer, stabilizer, reactive modifier, and diluent. ESO shows excellent promise as an inexpensive renewable material for industrial application [10, 11]. However, oil-based polymeric materials alone do not show sufficiently high properties of rigidity and strength required for different applications such as construction. In addition, bio-based thermoset polymeric materials have not been well studied. Therefore, in this study, we focus on the preparation and the effect of clay and hardener on the dispersion and properties of thermosets based on ESO.

EXPERIMENTAL

Materials

The bio-based resin selected for this study was ESO from St. Lawrence Chemical Inc., Canada. The hardeners were hexahydrophthalic anhydride and boron trifluoride monoethylamine (BF_3·MEA) from Sigma Aldrich Fine Chemicals. The nanoclays were sodium montmorillonite containing no organic intercalant (Cloisite® Na^+ from Southern Clay Products Inc., Gonzales, TX, USA), and three organo-nanoclays, namely Cloisite® 20A and Cloisite® 30B (montmorillonite treated with methyl tallow bis-(2-hydroxyethyl) quaternary ammonium), both also from Southern Clay Products, and Nanomer® I30E (montmorillonite treated with octadecyl amine, a primary amine base) from Nanocor Inc., Arlington Heights, IL, USA. Henceforth the hardeners and clay will be designated in shortened form as HHPA, BF_3, CNa, C20A, C30B, and I30E respectively.

Sample Preparation

Suspensions of ESO and clay were prepared using a mechanical mixer at 60°C for 10 minutes and the mixture was mixed thoroughly until cooled down to room temperature, then stored at room temperature. For curing, the required amount of hardener to obtain 2 wt% clay in the final product was mixed in at 120°C for at least 10 min and the mixture was then subjected to vacuum for another 5 min. Samples were cured at 160°C for 3 hours, with subsequent post cure at 200°C for another 2 hours. Rheological measurements were performed on ESO and ESO-clay suspensions with a strain-controlled rheometer, ARES (TA Instruments) at room temperature. The dynamic tests were carried out with 50 mm diameter parallel-plate geometry on suspensions stirred before loading in the rheometer. Infrared spectra were measured in ATR (attenuated total reflection) mode by means of a “Thunderdome” accessory from Thermo Spectra-Tech, equipped with a germanium reflection element. For molded samples, spectra were measured on a clean surface obtained by cutting with a blade. To evaluate the intercalation/exfoliation of the nanoclay in the polymer matrix, X-ray diffraction (XRD) patterns were obtained from the surface of the

samples with a Bruker Discover 8 powder X-ray diffractometer with CuKα radiation. A Hitachi-S4700 FEGSEM was used to observe the dispersion of clay in the ESO at the micro-level. To determine the T_g and to confirm the absence of any residual curing, the cured samples were heated in a TA- Q1000 DSC instrument using nitrogen atmosphere from -90°C to 100°C at 20°C·min^{-1}, then cooled to -90°C at 20°C·min^{-1} to minimize the enthalpy relaxation in the second heating scan, which involved reheating to 100°C at 20°C·min^{-1}. The hardness of epoxy and epoxy nanocomposites was determined at room temperature and relative humidity of 50% according to ASTM D2240-00 using a Shore Conveloader Instrument.

RESULTS AND DISCUSSION

Fig. 1 compares the complex viscosity of epoxy resin, ESO and the ESO-clay suspensions. The dynamic rheological measurements show that the ESO resin has Newtonian behavior with a viscosity value of 0.4 Pa·s in a frequency range of 1-100 s^{-1}. This viscosity value is very much lower than that of the Bisphenol A (epichlorohydrin) epoxy resin EPON 828 (E) with a viscosity of around 10 Pa·s. The mixture of 70 parts of ESO and 30 parts of EPON 828 (ESO7-E3) also shows a low viscosity of around 0.65 Pa·s (Fig. 1a). This is an advantage of ESO over EPON 828 in terms of processing, especially for resin transfer molding. The addition of clay does not change very much the viscosity and the rheological behavior of the ESO (Fig. 1b). The viscosity of ESO increases slightly from 0.41 Pa·s to 0.47 Pa·s with the presence of organoclays (ESO-2C20A, ESO-2C30B and ESO-2I30E). This may due to the dispersion of these organoclays in ESO. On the contrary, the viscosity of the ESO-2CNa suspension, in which the clay is not well dispersed, is even lower than that of the neat resin. The viscosity of ESO resin and ESO-clay suspensions remains constant with time for 2000 s, the length of the tests (results not shown here).

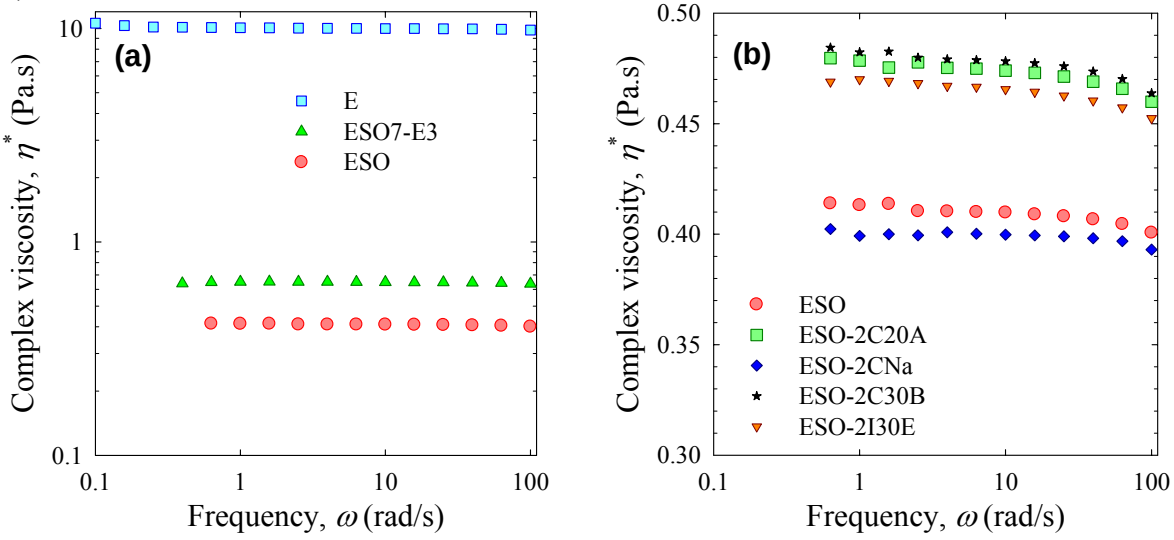

Fig. 1: Complex viscosity in function of frequency of: (a) EPON 828, ESO and the mixture of 70 parts of ESO and 30 parts of EPON 828, (b) ESO and ESO-clay suspensions.

Fig. 2 compares the infrared spectrum of neat uncured ESO with those of samples cured by homopolymerization through use of the catalyst BF_3. The ESO (Fig. 2a) shows a doublet at 841

and 823 cm^{-1} that does not appear in the spectrum of regular soyabean oil and presumably arises from the epoxide ring. Upon curing with BF_3 (Fig. 2b), these peaks disappear and are replaced by a strong band around 1085 cm^{-1} that corresponds to the ether groups formed upon homopolymerization. This confirms that cross-linking has occurred. The hydroxyl peak near 3500 cm^{-1} also increases somewhat in intensity. When nanoclay is present (Fig. 2c to 2f), the peak at 1085 cm^{-1} develops a shoulder around 1030 cm^{-1} that is due to the Si–O vibrations of the clay. Apart from this there is little variation in the spectrum. The C–H stretching bands remain at 2925 and 2855 cm^{-1}, and the carbonyl band remains at 1743 cm^{-1}. Fig. 3 shows the results obtained for ESO cured with HHPA. The HHPA itself (Fig. 3a) shows a strong anhydride ring band at 1785 cm^{-1} and a weaker one at 1856 cm^{-1}, while the ESO (Fig. 3b) shows epoxide ring peaks at 841 and 823 cm^{-1}. Upon reaction between the two (Fig. 3c), these peaks disappear almost completely, indicating a high degree of reaction. Compared to the neat ESO, the ester carbonyl peak becomes significantly broader and shifts to somewhat lower wavenumber; this is due to the presence of new ester groups from the epoxy-anhydride reaction (peak at around 1730 cm^{-1}) in addition to those initially present in the oil (peak at 1743 cm^{-1}). The samples containing nanoclay (Fig. 3d to 3f) give similar spectra. The clay peaks at 1050-1000 cm^{-1} are not obvious because they are masked by the strong peaks of the matrix. The carbonyl peak also shows either a shoulder or a distinct peak of varying intensity at 1705 cm^{-1}. This is due to unreacted carboxylic acid groups arising from the HHPA.

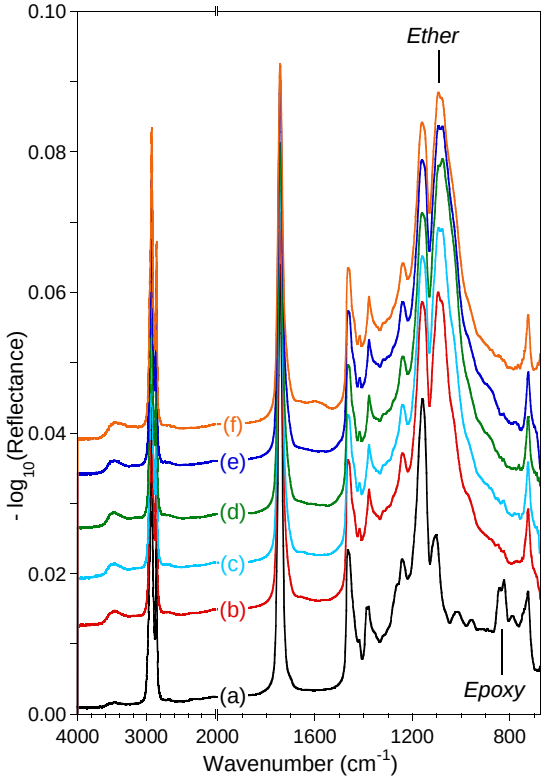

Fig. 2: IR spectra of: (a) ESO, and ESO cured with BF_3 catalyst and containing (b) no clay, (c) 2%CNa, (d) 2%C20A, (e) 2%C30B, or (f) 2%I30E.

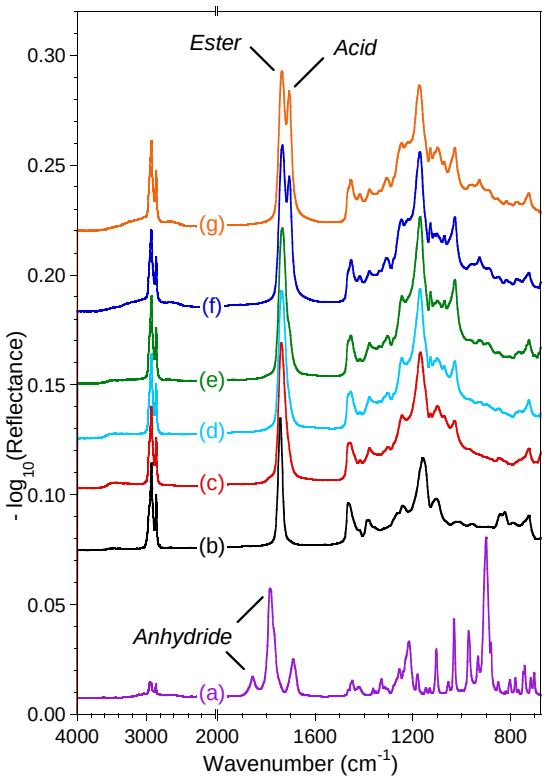

Fig. 3: IR spectra of: (a) HHPA, (b) ESO, and ESO cured with HHPA and containing (c) no clay, (d) 2% CNa, (e) 2%C20A, (f) 2%C30B, or (g) 2%I30E.

XRD is widely used to determine the clay intercalation/exfoliation of polymer nanocomposites because of its simple sample preparation and easy-to-interpret results. In XRD curves, the peak location (peak at angle 2θ), which relates to the gallery distance, can indicate the degree of intercalation. The intensity of peaks or area under peaks, which relates to the amount or the size of clay stacks, can indicate the degree of exfoliation or the size of stacks. The X-ray diffraction curves of ESO containing different types of clay after pre-mixing (liquid) and in the nanocomposites (solid) prepared by curing with different hardeners are shown in Fig. 4.

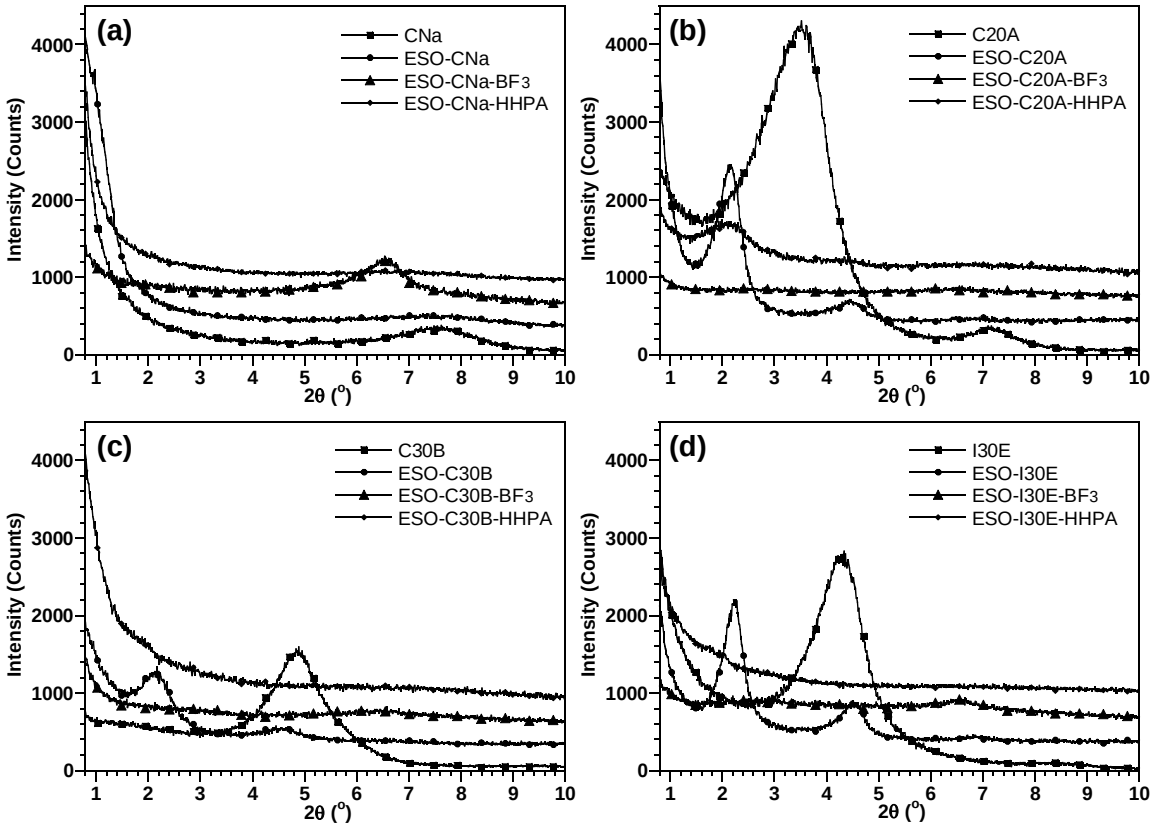

Fig. 4: X-ray diffraction curves of clay, ESO with clay, and their nanocomposites cured with BF_3 and HHPA: (a) CNa, (b) C20A, (c) C30B, and (d) I30E**.**

The results show that for the organoclays the peak shifts significantly to the left (smaller angle) but this is not the case for the sodium montmorillonite clay. The *d*-spacings of CNa, C20A, C30B, and I30E before mixing with ESO are 1.17, 2.42, 1.85 and 2.28 nm, respectively, and after mixing with ESO they are 1.18, 4.04, 4.07 and 3.97 n. This indicates that the organoclays have been intercalated by the ESO. After curing with hardener, the XRD peak either shifts further toward a smaller angle or disappears, depending on the clay and the curing. This means that the clay galleries are further expanded by ESO and hardener during curing. Although the XRD peak disappears in some cases, it is not clear whether the clays have been completely exfoliated or not. This is a limitation of XRD and it is necessary to confirm by SEM and TEM.

The microstructures of nanocomposite samples observed by FEGSEM are shown in Fig. 5. The bright spots on the backscattered images correspond to clay aggregates. Apparently, a portion of the clay remains at the micro-scale level with different size populations depending on the type of hardener and clay. As can be seen in Fig. 5a to 5d (samples cured with BF_3), there is a greater density of small particles for the C20A (Fig. 5b) than for the CNa (Fig. 5a), the C30B (Fig. 5c), and the I30E (Fig. 5d) in the ESO nanocomposite systems. This means that the C20A clay has been dispersed better compared to CNa, C30B, and I30E. The same trend was observed for the nanocomposites cured with HHPA. This indicates that the chemistry of the clay (intercalant) and hardener has a strong effect not only on the intercalation (as identified by XRD), but also on the dispersion of the clay at the micro level in the ESO. From the visual evidence of remaining micro aggregates, it is clear that the clays were not completely exfoliated in the ESO systems. The result also shows a better dispersion of clay in ESO cured with HHPA (Fig. 5e and 5f) compared to the corresponding samples cured with BF_3 (Fig. 5a and 5b).

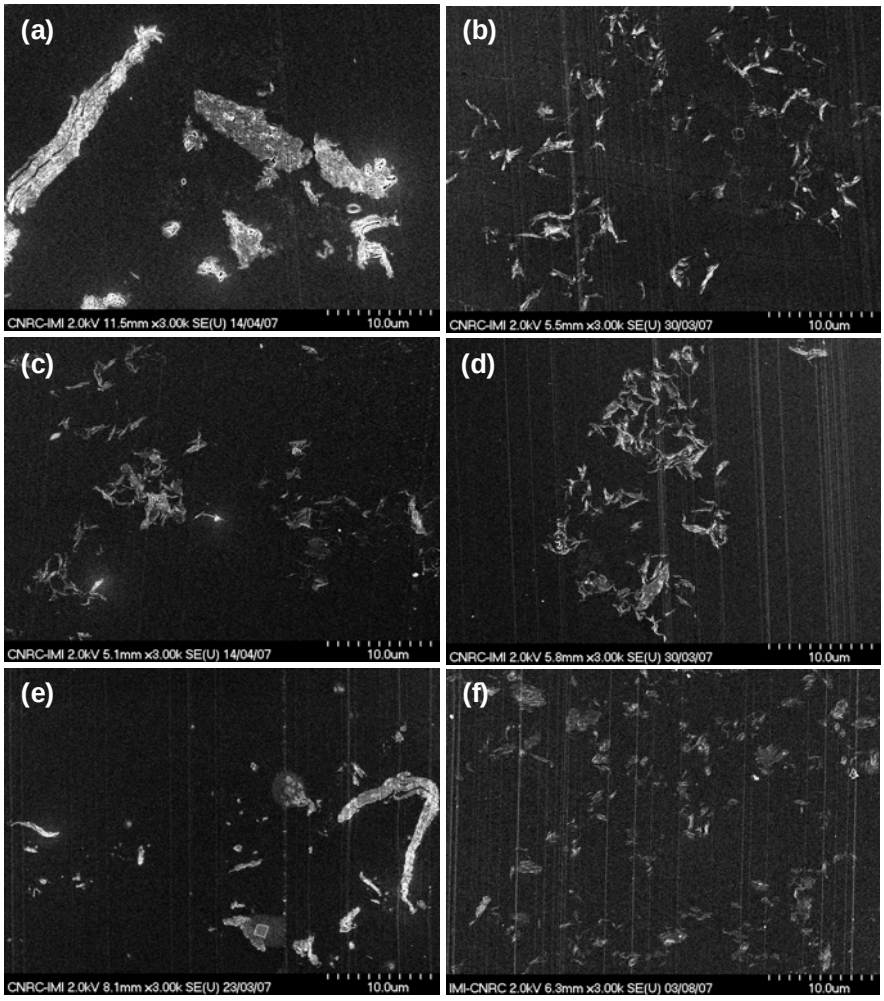

Fig. 5: SEM photos for ESO nanocomposites with different clays cured with BF_3 (a) CNa, (b) C20A, (c) C30B, (d) I30E and cured with HHPA (e) CNa, (f) C20A.

The surface hardness of the samples with and without clay was determined at room temperature and the results are shown in Fig. 6. As expected, adding nanoclay increases the surface hardness for cured ESO. However, the level of increase in the hardness is quite different depending on the clay type and the curing agent. Clay has a much greater surface hardness because of its ceramic nature. Therefore, it tends to contribute to the surface hardness of ESO. Furthermore, the better dispersion and better intercalation/exfoliation of the clay in the system may also be a contributing factor. For instance, the ESO nanocomposites based on C20A for both curing with BF_3 and HHPA have greater surface hardness compared to C30B, I30E and CNa.

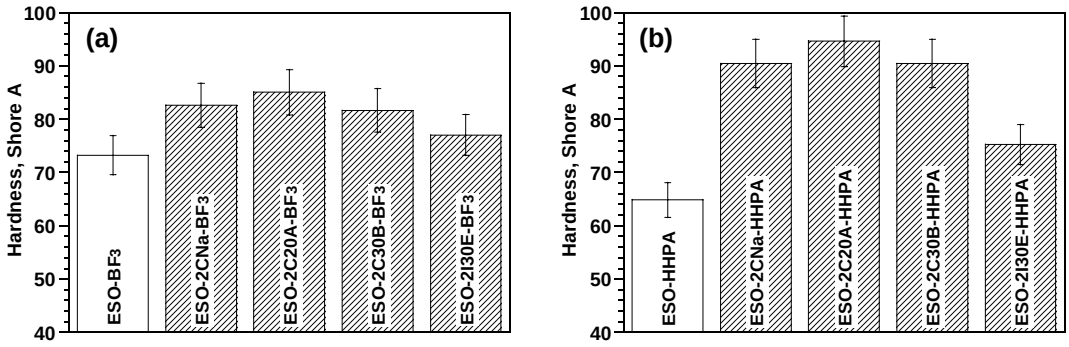

Fig. 6: Surface hardness for ESO and its nanocomposites cured with (a) BF_3 and (b) HHPA**.**

The T_g values of cured ESO and cured ESO nanocomposites were determined by DSC and the results are shown in Table 1. It was observed that the presence of clay and the type of clay do not have a strong effect on the T_g of the ESO cured with either BF_3 or HHPA. C30B, a montmorillonite treated with methyl tallow bis-(2-hydroxyethyl) quarternary ammonium, might be expected to undergo some interaction (for example hydrogen bonding) with the ESO and HHPA at the temperatures used in the study. Such interaction could result in an increase in the T_g of the system. C20A is a montmorillonite treated with dimethyl di(hydrogenated tallow) quaternary ammonium. The increase in the T_g correlates with the increase in surface hardness of the ESO when the clays are present.

Table 1: T_g values for ESO and its nanocomposites cured with BF_3 and HHPA

Sample	**T_g (°C)**	**Sample**	**T_g (°C)**
Cured with BF_3		*Cured with HHPA*	
ESO-BF_3	-20.2 ± 0.4	ESO-HHPA	-21.7 ± 0.7
ESO-2CNa-BF_3	-19.7 ± 0.5	ESO-2CNa-HHPA	-19.7 ± 0.7
ESO-2C20A-BF_3	-18.6 ± 0.4	ESO-2C20A-HHPA	-18.2 ± 0.4
ESO-2C30B-BF_3	-19.4 ± 0.5	ESO-2C30B-HHPA	-19.2 ± 0.4
ESO-2I30E-BF_3	-19.7 ± 0.6	ESO-2I30E-HHPA	-19.6 ± 0.6

CONCLUSION

Bio-based thermoset nanocomposites based on ESO reinforced with nanoclay particles have been studied. The dispersion of nanoclay in ESO varies depending on the type of clay and the hardener. Although the clay does not have a strong influence on the T_g of ESO, it does have a strong effect on the surface hardness of ESO nanocomposites.

ACKNOWLEDGEMENTS

T.-D. Ngo acknowledges a post-doctoral fellowship and Weawkamol Leelapornpisit acknowledges funding (Grant N00784 – Development of Bio-based Polymer Nanocomposites) from the Natural Sciences and Engineering Research Council of Canada. We also thank St. Lawrence Chemical Inc. for the ESO.

REFERENCES

1. A. Cunningham, and A. Yapp, Liquid Polyol Compositions, *U.S. Patent 3,827,993*, 1974.

2. G. W. Bussell, Maleinized Fatty Acid Esters of 9-Oxatetracyclo 4.4.1 O O Undecan-4-OL, *U.S. Patent 3,855,163*, 1974.

3. L. E. Hodakowski, C. L. Osborn, and E. B. Harris, Polymerizable Epoxide-Modified Compositions, *U.S. Patent 4,119,640*, 1975.

4. D. J. Trecker, G. W. Borden, and O. W. Smith, Method for Curing Acrylated Epoxidized Soybean Oil Amine Compositions, *U.S. Patent 3,979,270*, 1976.

5. D. J. Trecker, G. W. Borden, and O. W. Smith, Acrylated epoxidized Soybean Oil Amine Compositions and Method, *U.S. Patent 3,931,075*, 1976.

6. D. K. Salunkhe, J. K. Chavan, R. N. Adsule, and S. S. Kadam, World Oilseeds: Chemistry, Technology, and Utilization, *Van Nostrand Reinhold*, New York, 1992.

7. C. G. Force, and F. S. Starr, Vegetable Oil Adducts as Emollients in Skin and Hair Care Products, *U.S. Patent 4,740,367*, 1988.

8. D. P. Mishra, P. A. Mahanwar, Advances in Bioplastic Materials, *Pop Plast Packag*, **45** (7), 68-76, 2000.

9. J. Schroeter, Biodegradable Plastic Materials, *Kunststoffe*, **90** (1), 64-6, 2000

10. D. L. Kaplan, Biopolymers from Renewable Resources, *Springer-Verlag*, Berlin, p. 267, 1998.